

**Human GPRC6A mediates testosterone-induced ERK and mTORC1 signaling
in prostate cancer cells**

**Ruisong Ye, Min Pi, Mohammed M. Nooh, Suleiman W. Bahout,
and L. Darryl Quarles**

Department of Medicine (RY, MP, LDQ) and Pharmacology (SWB), The University of
Tennessee Health Science Center, 19 S Manassas St. Memphis, TN, 38163;
Department of Biochemistry (MMN), Faculty of Pharmacy Cairo University, Kasr El-Aini St.,
Cairo 11562, Egypt

Running title: Function of the human GPRC6A^{ICL3-KGKY} polymorphism

Correspondence:

Min Pi, Department of Medicine, University of Tennessee Health Science Center, 19 S
Manassas St. Memphis, TN 38163. Phone: 1-901-448-1458, Fax: 1-901-448-1188; E-mail:
mpi@uthsc.edu.

L. Darryl Quarles, Department of Medicine, University of Tennessee Health Science Center,
19 S Manassas St. Memphis, TN 38163. Phone: 1-901-448-1459, Fax: 1-901-448-1188; E-
mail: dquarles@uthsc.edu.

Number of text pages: 44

Number of tables: 0

Number of figures: 5

Number of references: 53

Number of words:

Abstract: 246

Introduction: 548

Discussion: 1050

Abbreviations: 4E-BP1, eukaryotic translation initiation factor 4E binding protein 1; AKT, protein kinase B; eIF4G, eukaryotic translation initiation factor 4G; ERK, Mitogen-activated protein kinases; AR, androgen receptor; GAPDH, glyceraldehyde 3-phosphate dehydrogenase; GPCR, G protein-coupled receptor; GPRC6A, G protein-coupled receptor family C group 6 member A; ICL3, third intracellular loop; LC3B, autophagy marker Light Chain 3; mTOR, mammalian target of rapamycin; mTORC1, mammalian target of rapamycin complex 1; RSK, 90 kDa ribosomal S6 kinases; S6, S6 ribosomal protein; S6K, p70S6 kinase; T, testosterone; TSC2, tuberous sclerosis complex 2; ULK1, Unc-51 like autophagy activating kinase 1.

Conflict of interest: The authors declare that they have no conflicts of interest with the contents of this article.

ABSTRACT

GPRC6A is activated by testosterone and modulates prostate cancer (PCa) progression. Most humans have a GPRC6A variant that contains a recently evolved KGKY insertion/deletion in the third intracellular loop (ICL3) (designated GPRC6A^{ICL3_KGKY}) that replaces the ancestral KGRKLP sequence (GPRC6A^{ICL3_RKLP}) present in all other species. *In vitro* assays purport that human GPRC6A^{ICL3_KGKY} is retained intracellularly and lacks function. These findings contrast with ligand-dependent activation and coupling to mTORC1 signaling of endogenous human GPRC6A^{ICL3_KGKY} in PC-3 prostate cancer cells. To understand these discrepant results, we expressed mouse (mGPRC6A^{ICL3_KGRKLP}), human (hGPRC6A^{ICL3_KGKY}) and “humanized” mouse (mGPRC6A^{ICL3_KGKY}) GPRC6A into HEK-293 cells. Our results demonstrate that the mGPRC6A^{ICL3_KGRKLP} acts as a classical GPCR that is expressed at the cell membrane and internalizes in response to ligand activation by testosterone. In contrast, hGPRC6A^{ICL3_KGKY} and “humanized” mouse mGPRC6A^{ICL3_KGKY} are retained intracellularly in ligand naive cells, yet exhibit β -arrestin dependent signaling responses, ERK and S6K phosphorylation in response to testosterone, indicating that hGPRC6A^{ICL3_KGKY} is functional. Indeed, testosterone stimulates time- and dose-dependent activation of ERK, AKT and mTORC1 signaling in wild-type PC-3 cells that express endogenous GPRC6A^{ICL3_KGKY}. In addition, testosterone stimulates GPRC6A-dependent cell proliferation in wild-type PC-3 cells and inhibits autophagy by activating mTORC1 effectors 4E-BP1 and ULK1. Testosterone activation of GPRC6A has the obligate requirement for calcium in the incubation media. In contrast, in GPRC6A deficient cells, the

effect of testosterone to activate down-stream signaling is abolished, indicating that human GPRC6A is required for mediating the effects of testosterone on cell proliferation and autophagy.

Keywords: GPRC6A, testosterone, mTORC1, AKT, ERK, proliferation, autophagy

INTRODUCTION

GPRC6A is a member of the class-C GPCR family that is widely expressed and activated by multiple ligands, including the peptide osteocalcin (Ocn), cations, basic amino acids and testosterone (Pi et al., 2017). The linkage of a venus fly trap motif (VFTM) to the classical GPCR 7-transmembrane domain accounts for the ligand diversity of GPRC6A (Pi et al., 2015; Pi et al., 2018a; Pi et al., 2012). Mouse GPRC6A is proposed to regulate complex endocrine networks and metabolic processes, as demonstrated in *in vitro* cell culture and *in vivo* animal models (Ferron et al., 2010; Karsenty and Olson, 2016; Pi et al., 2016; Pi et al., 2017). Genetic loss-of-function studies and pharmacological activation of GPRC6A in mice show that GPRC6A regulates insulin secretion and proliferation by β -cells (Oury et al., 2013; Pi et al., 2012; Pi et al., 2011; Wei et al., 2014), glucose uptake and IL-6 secretion by skeletal muscle (Mera et al., 2016), testosterone secretion by testicular Leydig cells (De Toni et al., 2014), glucose and fat metabolism by hepatocytes and adipocytes (Otani et al., 2015) and prostate cancer progression (Pi and Quarles, 2012). GPRC6A in these tissues senses Ocn released from bone to create endocrine networks regulating energy homeostasis and sexual reproduction (Pi et al., 2017). GPRC6A also mediates the rapid, non-genomic, effects of testosterone in peripheral tissues, including Leydig cells, β -cells, skeletal muscle, and skin keratinocytes (Ko et al., 2014; Pi et al., 2015; Pi et al., 2010).

A KGKY polymorphism in the third intracellular loop (ICL3) of GPRC6A evolved in most humans (GPRC6A^{ICL3_KGKY}) (Jørgensen et al., 2017) to replace the ancestral KGRKLP

(GPRC6A^{ICL3_KGRKLP}, rs386705086) sequence present in all animal species. HEK-293 cells transfected with mouse GPRC6A^{ICL_KGRKLP} show that this ancestral variant localizes to the cell surface membrane, and imparts signaling responses to Ocn, testosterone, L-Arginine, and cations (Mera et al., 2016; Oury et al., 2013; Pi et al., 2005; Pi et al., 2015; Pi et al., 2018a; Pi et al., 2016; Pi et al., 2010; Pi et al., 2012; Ye et al., 2017). In contrast, human GPRC6A^{ICL3_KGKY} is proposed to be a loss-of-function polymorphism that is not associated with any human diseases (Jørgensen et al., 2017). Studies of a human cDNA transfected into HEK-293 cells found that the GPRC6A^{ICL3_KGKY} variant is retained intracellularly and lacks responsiveness to Ocn and testosterone (Jacobsen et al., 2017; Jørgensen et al., 2017). If this scenario is correct, a functional GPRC6A in humans would be limited to the 20% of Caucasians and 40% of people of African-descent that express the ancestral KGRKLP polymorphism (Pi et al., 2017).

In the current study, we determined the distribution of transfected mouse, human GPRC6A and “humanized” mouse GPRC6A^{ICL3_KGKY} constructs in naive and testosterone-stimulated HEK-293 cells. We also examined the function effects of GPRC6A ligands in wild-type PC-3 cells expressing endogenous GPRC6A^{ICL3_KGKY} and in cells after ablation of GPRC6A. We found that GPRC6A^{ICL3_KGRKLP} is cell surface expressed and imparts second messenger signaling and undergoes internalization in response to GPRC6A agonists, consistent with a classical GPCR. In contrast, we confirmed that GPRC6A^{ICL3_KGKY} is retained intracellularly, but leads to ERK and mTORC1 activation in response to ligands. Thus, the GPRC6A^{ICL3_KGKY} polymorphism is not a loss-of-function polymorphism but may have evolved to link to nutrient sensing to ERK and mTORC1 pathways after internalization to endosomes.

MATERIALS AND METHODS

Establishment of CRIPR/Cas9-Mediated GPRC6A KO cell clones

In the present study, one GPRC6A KO single clone B12 was selected from our previously established CRISPR/Cas9 -edited GPRC6A PC-3 cell line (Ye et al., 2017). We obtained a total of 11 single clones using serial dilution method, in which B12 contain 2nt insert (sequence was confirmed by T-A cloning sequencing) and cause frame-shift mutation and lost-of-function in response to ligands stimulation (detail see Fig. S1 and Fig. S2).

Cell culture and treatment

Cells were cultured in RPMI1640 media and cell proliferation assays as previously described (Ye et al., 2017). Briefly, 4×10^3 cells were seeded in the each well of 96-well plate, with or without 50 nM testosterone, and the MTT dye production method was used to measure for cell proliferation (Cayman Chemical, # 10009365). For treatment, cells were placed in Hank's Balanced Salt Solution (HBSS, Thermo Fisher Scientific #14175145, supplemented with 0.5mM Ca^{2+} , if not otherwise stated) for 2-3h before stimulation. For autophagy assay, we used GPRC6A KO (B12) and GPRC6A WT control cells (with Cas9 expression, without sgRNA expression) to examine LC3B level and phosphorylation of ULK1. Cell autophagy is induced by 5h starvation in HBSS with 50 μM chloroquine (Lee et al., 2007) . In addition, both GPRC6A

KO cells and control cells were transfected with RFP-LC3 expression plasmids and established stable cell lines, and the cells were further used for LC3 punctate measurement. Images were taken using a Nikon Ti inverted fluorescence microscope.

RT-PCR and Real-time PCR

The RT-PCR assay performed as previous studies (Pi et al., 2010). The primers used for RT-PCR and Real-time was listed in Table S1.

Western blot

Western blots were performed as previously described (Ye et al., 2017). Briefly, after 48 hours culture, quiescence was achieved in subconfluent cultures by removing the medium and washing with HBSS to remove residual serum, followed by incubation for an additional 4h in serum-free medium (DMEM/F-12 medium containing 0.1% BSA and about 1 mM calcium; Thermo Fisher Scientific #A322965). After agonist treatment at the specified concentrations and duration, cells were washed twice with ice-cold PBS and scraped into 250 μ l of LDS sample buffer (Thermo Fisher Scientific #NP0008) with 0.02 tablet/ml of protease inhibitor tablets (Thermo Fisher Scientific #11330). Equal amounts of lysates were subjected to 10% SDS-PAGE, target protein levels were determined by immunoblotting using antibodies. The

antibodies used for these analyses were listed in Table S2. Western blot intensity was analyzed by Image J software.

Confocal microscopy procedures

Cells stably expressing myc-tagged mouse WT GPRC6A (mGPRC6A^{ICL3_KGRKLP}) or myc-tagged mouse GPRC6A^{ICL3_KGKY} were cultured in DMEM + 10% FBS supplemented with 200 µg/ml of G418. Cells plated on laminin-coated glass coverslips were pre-exposed to buffer or to 30 µM Dyngo-4a for 30 min and then to 1 µM testosterone for an additional 30 min (Li et al., 2013). Thereafter, slides were fixed in phosphate-buffered saline containing 4% paraformaldehyde and 4% sucrose (pH 7.4) for 10 minutes at room temperature (Bahouth and Nooh, 2017). To permeabilize the cells, fixed slides were incubated in HEPES-buffered saline solution containing 0.2% Triton X-100 for 10 minutes at 4°C, followed by three washes in ice-cold PBS (Li et al., 2013). At this stage, coded slides were blocked with 5% bovine serum albumin in PBS for 30 min at room temperature. Cells expressing mGPRC6A^{ICL3_KGRKLP} or mGPRC6A^{ICL3_KGKY} were incubated with 1:250 dilution of monoclonal anti-9E10 c-Myc antibody in PBS or in 5% FBS in PBS for permeabilized cells for 1 h at room temperature. Similarly, cells expressing human GPRC6A (hGPRC6A^{ICL3_KGKY}) were incubated with 1:250 dilution of rabbit anti-GPRC6A antibody in PBS for non-permeabilized cells and in 5% FBS in PBS for permeabilized cells. Cells expressing mGPRC6A^{ICL3_KGRKLP} or mGPRC6A^{ICL3_KGKY} were incubated with 1:250 dilution of goat anti-mouse IgG conjugated to Alexa Fluor 555, while cells

expressing hGPR6CA were incubated in 1:500 dilution of CF-633 conjugated to Donkey anti-rabbit IgG for 1h at room temperature. These antibodies were diluted in PBS for non-permeabilized cells or in PBS containing 5% FBS for permeabilized cells. The slides were washed 3 times in PBS and then mounted on microscopic glass slides for confocal microscopy. Confocal fluorescence microscopy was performed at room temperature on coded slides and optical section thicknesses of 1.0 mm images were acquired by an Olympus FV1000 confocal microscope equipped with 40 or 60 Å oil immersion (numerical aperture 1.30) objective lens, using FV10-ASW 3.1 acquisition soft-ware (Olympus, Center Valley, PA) (Bahouth and Nooh, 2017). TIFF files of each image were exported and analyzed for pixel intensity and distribution by *ImageJ* software (<https://imagej.nih.gov/ij/>). Each cell was partitioned by a line, every point of which was at a distance of 300 nm from the outer periphery of the cell, using the *ImageJ* software. This line formed the outer limit of the area used to index pixel intensity of internal GPRC6A in a given cell, while the area formed between the peripheral cell membrane and this line was used to index the distribution of pixels associated with cell surface GPRC6A (Bahouth and Nooh, 2017; Gardner et al., 2007; Li et al., 2013).

Statistics

Data were derived from image analysis that determined specific total pixels and pixels outside versus inside the 300-nm partition that was drawn around the inner circumference of cardiomyocytes. The ratio of pixels residing outside the 300-nm partition to that of the

percentage of total pixels was calculated for each image. The average \pm S.E. of percentile pixel ratios from three separate experiments derived from 10 images/experiment (n = 30 images) is presented. Statistical comparison between two groups was performed by unpaired *t* tests and for multiple groups by analysis of variance (Tsvetanova and von Zastrow, 2014) followed by Bonferroni's test with a single pooled variance test in which the family-wise error rate was set at 0.05, using GraphPad Prism 7 software (GraphPad Software Inc.). Regarding the data of western blot, cell proliferation and autophagy assay, the statistical significance of differences between the two groups was calculated by using Student's *t* test. Other statistical analyses performed were Dunnett's or Tukey-Kramer's tests, as post-hoc tests following the analysis of variance (ANOVA).

RESULTS

Dose and time dependence of testosterone-mediated activation of ERK/PI3K/Akt/mTORC1 signaling in PC-3 cells that express the endogenous GPRC6A^{ICL3_KGKY} polymorphism

PC-3 cells endogenously express human GPRC6A^{ICL3_KGKY} but not androgen receptor (AR) transcripts (Ye et al., 2017), making them a model to study the non-genomic, AR-independent effects of testosterone (Fig. 1A). The human prostate cancer cell, 22RV1 highly expressed GPRC6A and AR (Pi and Quarles, 2012), we used 22RV1 cells as the positive control. To create a PC-3 cell line with ablated GPRC6A, we used CRISPR/Cas9 system to delete the hGPRC6A gene (Fig. S1 and S2). We selected a PC-3 cell clone, termed B12 (PC-3/GPRC6A^{KO-B12}), which lacked the mRNA and protein of hGPRC6A (Fig. 1B-C) and used it along with wild-type PC-3 cells to determine if ablation of hGPRC6A was associated with loss of down-stream signaling by testosterone.

We found that the testosterone dose-dependently activated ERK and S6K phosphorylation in wild-type human PC-3 cells expressing GPRC6A^{ICL3_KGKY} (Fig. 1D, *left panel*), and this response was lost in PC-3/GPRC6A^{KO-B12} cells (Fig. 1D, *right panel*), indicating that human GPRC6A was required for testosterone-mediated signaling responses in PC-3 cells. Next, we tested the more specific AR ligand DHT that is derived from 5-alpha-reductase conversion of testosterone and in previous studies has been shown not to activate GPRC6A

(Pi et al., 2010). DHT failed to induce phosphorylation of ERK or S6K in PC-3 cells at concentrations ranging from 1 to 100 nM (Fig. 1E), consistent with the notion that PC-3 cells lack AR and in agreement with previous results showing that testosterone but not DHT activated down-stream signaling by the hGPCR6A (Pi et al., 2015).

Because the VFT and 7-TM structures of GPCR6A predicts activation by cations and allosteric modulators, we reexamined if Ca^{2+} is required for testosterone-mediated activation of hGPCR6A (Oury et al., 2013; Pi et al., 2010; Wellendorph and Bräuner-Osborne, 2009; White et al., 2013). For these studies, PC-3 cells were incubated in a buffer with or without 0.5 mM Ca^{2+} and then exposed to testosterone. We found that testosterone failed to induce phosphorylation of ERK, AKT, S6K or S6 signaling in the buffer without Ca^{2+} (Fig. 1F). Ca^{2+} alone weakly stimulated phosphorylation of these down-stream signals, but the effects of testosterone on Ca^{2+} were additive, leading to a robust induction of phosphorylation, as previously reported (Pi et al., 2010).

The time-course of testosterone-mediated activation of endogenous hGPCR6A was rapid in onset. We observed increased phosphorylation of both ERK and AKT within 2 min with maximal activation by 10 min that was sustained throughout the 30-minute observations period (Fig. 2A).

ERK and AKT are upstream of mTORC1 (Mendoza et al., 2011), an evolutionarily conserved nutrient sensing pathway (Ben-Sahra and Manning, 2017; Efeyan et al., 2012). Phosphorylation of p70S6 kinase (S6K) at Thr389, S6 ribosomal protein (S6) at Ser235/236, eukaryotic translation initiation factor 4E binding protein 1(4E-BP1) at Ser65 are characteristic

downstream markers for activation of the mTORC1 pathway (Mendoza et al., 2011). Testosterone at concentrations of 50 nM time-dependently increased the phosphorylation of pS6K-Thr389, pS6-Ser235/236 and p4E-BP1-Ser65, and their phosphorylation was activated as early as 2 minutes (Fig. 2B).

To further confirm that ERK and AKT mediated testosterone induced-mTORC1 activation, PC-3 cells were treated with testosterone in the presence of PD98059 (ERK inhibitor), and/or MK2206 (AKT inhibitor). Testosterone induced-mTORC1 activation was partially blocked by the ERK inhibitor (PD98059) and completely inhibited by the AKT inhibitor (MK2206) (Fig. 2C). Treatment with the potent AKT inhibitor MK2206 completely inhibited AKT-S473 phosphorylation, but not ERK phosphorylation. In addition, MK2206 inhibited the phosphorylation of ribosomal protein S6 at pS6K-T389 and pS6-S235/236, which is a downstream target of mammalian target rapamycin 1 (mTORC1) activation (Fig. 2C). PD98059 completely blocked ERK phosphorylation, but had no effect on AKT phosphorylation, and partially inhibited ribosomal protein S6 phosphorylation (Fig. 2C). Rapamycin, an mTOR inhibitor, blocked testosterone-induced ribosomal protein S6 phosphorylation in PC-3 cells without affecting ERK or AKT phosphorylation (Fig. 2C and 2D).

To define pathways between ERK and AKT activation of mTORC1, we examined the effects of testosterone on phosphorylation of tuberous sclerosis complex 2 (TSC2) and MAPK-activated protein kinase RSK (p90 ribosomal S6 kinase). Testosterone significantly stimulated RSK phosphorylation in PC-3 cells, and this response was completely blocked by the ERK inhibitor, partially inhibited by rapamycin, and not affected by the AKT inhibitor. Conversely,

testosterone also induced TSC2 phosphorylation at Thr1462 and this response was blocked by the AKT inhibitor but not the ERK inhibitor (Fig. 2D). These findings suggest that ERK/RSK and AKT are two independent pathways involved in testosterone-induced mTORC1 activation in PC-3 cells.

GPRC6A regulates cell proliferation and autophagy through mTORC1 signaling

Since mTORC1 is a master regulator of cell growth, metabolism, and survival (Laplante and Sabatini, 2009), we determined the role of mTORC1 in mediating the function of hGPRC6A in PC-3 cells.

First, we examined the effects of testosterone on cell survival and proliferation in wild-type PC-3/GPRC6A^{IC3_KGKY} and in the GPRC6A knockout PC-3/GPRC6A^{KO-B12} cell lines. These cells were seeded at the same density and incubated for two days in the presence or absence of testosterone (Cvicek et al.). We consistently counted fewer PC-3/GPRC6A^{KO-B12} cells compared to wild-type PC-3 cells hGPRC6A lead to impaired cell proliferation and/or decreased survival. We speculate that these effects were mediated by hGPRC6A, because testosterone significantly increased the number of cell in wild-type PC-3 cells expression the endogenous GPRC6A^{IC3_KGKY} variant but not in PC-3/GPRC6A^{KO-B12} cells (Fig. 3A). Testosterone also induced expression of the cell proliferation marker Ki-67 (Fig. 3B) and induced the phosphorylation of 4E-BP1 and eIF4G, two effectors of mTORC1 signaling that are responsible for regulating the proliferation of PC-3/GPRC6A^{IC3_KGKY} cells. However, in

hGPRC6A-null PC-3 (PC-3/GPRC6A^{KO-B12}) cells, the effect of testosterone on these parameters was completely abolished (Fig. 3B).

Next, we examined if human GPRC6A was involved in regulating autophagy in PC-3 cells because mTORC1 is a major inhibitor of autophagy, and testosterone has been shown to inhibit autophagy (Tomaszewski et al., 2015). Since mTORC1 suppressed autophagy via phosphorylating Unc-51 like autophagy activating kinase-1 ULK1 at Ser757, we examined if testosterone would further increase the phosphorylation of ULK-1 on Ser757. Testosterone induced a time dependent increase in the phosphorylation of ULK-Ser757, achieving a maximal response by 30 minutes (Fig. 3C). Testosterone-mediated increase in the phosphorylation of ULK-Ser757 was observed in wild-type or PC-3/GPRC6A^{IC3_KGKY} cells, but not in GPRC6A null PC-3/GPRC6A^{KO-B12} cells (Fig. 3D).

The autophagy-related protein LC3 is a widely used marker of autophagosomes, where the lipidated form of LC3-II indexes autophagic activity (Yoshii and Mizushima, 2017). Western blot analysis showed that phosphorylation of lipidated LC3 (LC3II) was decreased after testosterone stimulation, in PC-3/GPRC6A^{IC3_KGKY} cells, whereas basal phosphorylation was increased in vehicle treated PC-3/GPRC6A^{KO-B12} cells that exhibited no response to testosterone (Fig. 3D). PC-3/GPRC6A^{KO-B12} cells also exhibited increased formation of LC3 autophagosomes, while testosterone reduced LC3-II expression in PC-3/GPRC6A^{IC3_KGKY} cells, an effect blocked by deletion of GPRC6A blocked in PC-3/GPRC6A^{KO-B12} (Fig. 3E).

Collectively, these results unequivocally establish the function of endogenous human GPRC6A^{IC3_KGKY}, and contrast with the reported lack of function of a transfected hGPRC6A

construct, which was found to be retained intracellularly (Jørgensen et al., 2017). We propose that hGPCR6A is an example of a GPCR that exhibits ligand-dependent signaling after endocytosis (Cahill et al., 2017; Thomsen et al., 2016).

Cellular localization and ligand dependent activation of the GPCR6A KGKY and RKLP polymorphisms.

To examine the impact of the KGKY and KGRKLP motifs on ligand-dependent endocytosis, we transfected WT human GPCR6A (GPCR6A^{ICL3_KGKY}), Myc-tagged WT mouse GPR6CA (GPCR6A^{ICL3_KGRKLP}) and Myc-tagged “humanized” mouse GPCR6A (Myc-mGPCR6A^{ICL3_KGKY}), which was created by replacing KGRKLP with KGKY in the 3rd ICL of mGPCR6A into HEK-293 cells. The cells were fixed and then either used as such or were permeabilized as described in the Methodology section. The cells were then incubated with primary monoclonal (9E10) anti-Myc or rabbit anti-human GPR6CA antibodies, followed by secondary fluorescent anti-mouse or anti-rabbit IgG. Confocal fluorescence microscopy indicated that in HEK-293 cells, ancestral mGPCR6A (GPCR6A^{ICL3_KGRKLP}) pixels were predominately located (70 ± 14%) in the cell surface membrane of intact or permeabilized HEK-293 cells (Fig. 4A, *images a and b*, respectively). In contrast, in HEK-293 cells, humanized mouse GPCR6A (mGPCR6A^{ICL3_KGKY}) (Fig. 4A, *images c and d*) or human GPCR6A (Fig. 4A, *images e and f*) were mostly intracellular. These receptors were distributed by ~ 12% and 17% on the cell

surface and by 88 ± 17 and $83 \pm 15\%$ internally (Fig. 4B), respectively ($n = 30$ images derived from three separate experiments).

Consistent with findings in classical GPCR, activation of mGPRC6A with testosterone induced the redistribution of the pixels from the membrane to internal puncta that had a diameter of 300-500 nm, commonly associated with endosomal structures (Fig. 5A, *images a and b*). In contrast, addition of testosterone, which activates hGPRC6A, did not alter the distribution of internal humanized mGPRC6A (GPRC6A^{ICL3_KGKY}) (Fig. S3).

Translocation of mGPRC6A in response to testosterone was inhibited in cells pretreated with the potent dynamin inhibitor Dyngo-4a (Robertson et al., 2014) (Fig. 5A, *image c*). To confirm Dyngo-4a blocks mGPRC6A-mediated testosterone-induced translocation and function, we compared the functions of mGPRC6A and hGPRC6A in testosterone-induced intracellular ERK phosphorylation. In contrast, we found that Dyngo-4a enhanced testosterone-induced ERK phosphorylation in mGPRC6A, but inhibited testosterone-induced ERK activity in hGPRC6A transfected HEK-293 cells (Fig. 5B).

β -arrestins are multifunctional endocytic adaptors and signal transducers (Lefkowitz and Shenoy, 2005). Next, we studied if β -arrestins are involved in GPRC6A endocytosis using β -arrestin inhibitor, Barbadin (Beautrait et al., 2017). Like Dyngo-4a, Barbadin (10 μ M) enhanced testosterone-induced ERK phosphorylation in mGPRC6A transfected HEK-293 cells, but inhibited testosterone-induced ERK phosphorylation in hGPRC6A transfected HEK-293 cells (Fig. 5C, upper panel). Interestingly, Barbadin also increased activation of S6K in mGPRC6A,

but decreased S6K phosphorylation in hGPCR6A transfected HEK-293 cells (Fig. 5C, middle panel).

These findings are consistent with prior studies showing desensitization of mouse GPCR6A signaling through a β -arrestin dependent classical rapid recycling mechanism, and findings of Jorgensen et al. showing that the KY insertion/deletion in GPCR6A is “mostly” retained intracellularly (Jørgensen et al., 2017) and recycles through a β -arrestin-dependent slow recycling mechanism (Lefkowitz and Shenoy, 2005; Pi et al., 2005).

Finally, we compared the effect of KGKY on Western blot migration of epitope tagged mGPCR6A, “humanized” mouse GPCR6A and human GPCR6A using Myc antibody. The estimated molecular weight of the GPCR6A monomer is 110 kDa, and GPCR6A is known to form a dimer with a molecular weight of ~ 220 kDa (Norskov-Lauritsen et al., 2015; Ye et al., 2017). We found that the human GPCR6A dimerized to a lesser extent compared to the mouse GPCR6A as evidenced by an altered distribution of GPCR6A monomers and dimers in HEK-293 cells transfected with these constructs (Fig. 5D). Interestingly, both wild-type mouse mGPCR6A^{ILC3_KGRKLP} and the “humanized” mGPCR6A^{ILC3_KGKY} showed equal amounts of 110 kDa and 220 kDa protein bands, corresponding to monomer and dimer migration (1.23 or 1.18, dimer/monomer ratio, respectively), whereas the wild-type human GPCR6A^{ILC3_KGKY} showed greater ratio of monomer to dimer (0.32 dimer/monomer ratio), suggesting that the polymorphisms in the 3rd ICL is not controlling dimerization (Fig. 5D).

DISCUSSION

A newly evolved human GPRC6A orthologue with the ICL3_KGKY polymorphism is reported to be retained intracellularly and to lack ligand-dependent activation (Jørgensen et al., 2017). These negative findings, along with failure to identify any association between GPRC6A mutations and human diseases in a Danish cohort, have raised questions about the biological relevance of GPRC6A in humans. Our data, however, shows that human GPRC6A^{ICL3_KGKY} variant, though predominantly intracellular, can be detected in the plasma membrane, and more importantly is functional as evidence by its activation by testosterone and other agonists, as previously reported (Pi et al., 2018a; Pi et al., 2016; Pi et al., 2018b).

The current studies extend our understanding of the important difference between GPRC6A membrane locations imparted by replacement of the ancestral RKLP sequence with the KGKY insertion/deletion in the 3rd ICL. We show that the mouse GPRC6A with the ancestral RKLP polymorphism in the 3rd ICL acts like a classical GPCR in that mGPRC6A is predominately expressed in the cell surface membrane and undergoes ligand-dependent internalization, perhaps via clathrin-coated pit-mediated endocytosis. On the other hand, human GPRC6A^{ICL3_KGKY} is present in low levels in the cell membrane (~20%) and is predominately located (~80%) in the endosome-like intracellular punctuate structures, consistent with the observation that human GPRC6A is largely retained intracellularly and undergoes slow recycling from the endosome (Jacobsen et al., 2017). The molecular mechanism whereby replacing the KGRKLP sequence with KGKY leads to intracellular

retention needs further study. Since the KGRKLP motif is present in Family C members that undergo desensitization and recycling to the plasma membrane, it is tempting to speculate that the KGRKLP sequence represent a “membrane retention” motif, and the replacement with the KGKY motif leads to a loss-of-binding to essential proteins leading to GPCR cycling to endosomes (Lefkowitz and Shenoy, 2005).

Regardless, and most importantly, in contrast to the purported lack of ligand-dependent activation of a transfected human GPRC6A (Jørgensen et al., 2017), we found that endogenous human GPRC6A in PC-3 cells responds to the agonist testosterone by activating ERK and PI3K/AKT signaling pathways. More importantly, ligand activation of GPRC6A is linked to downstream mTOR activation. The cell surface expressed human GPRC6A may likely account for our previous observations showing that co-expression of β -arrestin 1 and 2, C3 toxin, or pertussis toxin pretreatment blocked the effects of cations to activate transfected human GPRC6A (Pi et al., 2005). The endosomal signaling by internalized GPRC6A is similar to the evolutionarily conserved pathway in which L-arginine activates mTORC1 signaling in lysosomes from yeast to mammals (Efeyan et al., 2012; Kapahi et al., 2010; Saxton and Sabatini, 2017). Similar to the lysosomal nutrient sensing pathway, testosterone activation of GPRC6A in the endosomes may also result in the inhibition of autophagy and induction of anabolic cellular responses through activation of S6 kinase and inhibition of repressor polypeptide 4E-BP1 and ULK1.

Our current findings are consistent with prior observations that “*humanizing*” the mouse GPRC6A by replacing the KGRKLP sequence with KGKY prolonged mTOR signaling,

suggesting the internalized KGKY polymorphism is a gain-of-function variant (Ye et al., 2017), but not consistent with the reported agonist-independent internalization and slow recycling from the endosome of human GPRC6A reported by others (Jacobsen et al., 2017).

The structural basis for sensing of cations, and L-Arginine residues in the VFT, and testosterone, Ocn and other ligands is imparted by the VFT and 7-TM domain structure (Pi et al., 2005; Pi et al., 2015; Pi et al., 2018a; Pi et al., 2016). The inability to show ligand-dependent activation of GPRC6A by other investigators may be due inclusion of a wash step that depleted essential co-factors necessary for ligand activation of GPRC6A. Consistent with this possibility, we found that testosterone activation of GPRC6A is dependent upon a media calcium concentration of at least 0.5 mM. Physiologically, GPRC6A is always in the presence of calcium above the activating threshold, whereas the concentrations of testosterone, Ocn and other ligands may vary to activate GPRC6A. Our studies examine the function of GPRC6A in PC-3 cells that do not express the AR; however, we have shown that GPRC6A has similar function in 22RV1 cells that express AR (Pi and Quarles, 2012).

Thus, rather than being a non-functional variant, human GPRC6A appears to belong to the growing examples of GPCRs that exhibit endosomal signaling after ligand-mediated internalization (Cahill et al., 2017; Thomsen et al., 2016). In the case of GPRC6A^{ICL3_KGKY} the internal signaling is linked to ERK and mTOR, suggesting that the KGKY polymorphism may have evolved to provide a means for a GPCR to activate mTORC1 in endosomes/lysosomes. Additional studies are needed to define the intracellular compartments in which GPRC6A activates mTOR signaling.

Regardless, the potential biological significance of GPRC6A is shown by studies of mouse GPRC6A indicate important roles in regulating energy metabolism and prostate cancer progression (Di Nisio et al., 2017; Oury et al., 2013; Pi et al., 2017; Pi et al., 2010; Pi and Quarles, 2012; Pi et al., 2011). GPRC6A antagonists would inhibit both AKT/mTOR and ERK/MAPK signaling, which is an effective methods for treating hormone-refractory PCa (Kinkade et al., 2008). If the human GPRC6A^{ICL3_KGKY} has similar functions to mouse GPRC6A, it may account for racial disparities in susceptibility to metabolic disorders and prostate cancer (Cho, 2011; Laplante and Sabatini, 2012).

Presently, clinical studies show that levels of the GPRC6A ligand, Ocn, are inversely associated with glycemic status, insulin resistance, and obesity in humans (Foresta et al., 2011; Iki et al., 2012; Pittas et al., 2009). Genome wide association studies (GWAS) find association with GPRC6A polymorphisms with insulin resistance (Di Nisio et al., 2017) testicular failure (De Toni et al., 2016; Oury et al., 2013) and prostate cancer (Long et al., 2012; Takata et al., 2010). A recent study of a Danish cohort, however, failed to identify any association between GPRC6A inactivating mutations and human disease (Jørgensen et al., 2017). GWAS analysis is confounded because the KGKY polymorphism is the referent sequence in humans and the RKLP polymorphism is not detected by current gene chips used to genotype patient cohorts.

In conclusion the emergence of GPRC6A^{ICL3_KGKY} only in hominids and its preservation during evolution indicates selection pressures that modified the functions of GPRC6A to

promote ligand-dependent intracellular signaling and coupling to ERK and mTOR. Further studies are needed to establish the clinical relevance of GPRC6A in human pathophysiology.

Acknowledgments:

We acknowledge Dr. Malia B. Potts for gifting GFP-RFP-LC-3 plasmid.

AUTHOR CONTRIBUTIONS

Participated in research design: Ye, Pi, and Quarles.

Conducted experiments: Ye, Pi, Nooh, and Bahout.

Performed data analysis: Ye, Pi, Bahout, and Quarles.

Wrote or contributed to the writing of the manuscript: Ye, Pi, Bahout, and Quarles.

REFERENCE

- Bahouth SW and Nooh MM (2017) Barcoding of GPCR trafficking and signaling through the various trafficking roadmaps by compartmentalized signaling networks. *Cellular signalling* **36**: 42-55.
- Beautrait A, Paradis JS, Zimmerman B, Giubilaro J, Nikolajev L, Armando S, Kobayashi H, Yamani L, Namkung Y, Heydenreich FM, Khoury E, Audet M, Roux PP, Veprintsev DB, Laporte SA and Bouvier M (2017) A new inhibitor of the beta-arrestin/AP2 endocytic complex reveals interplay between GPCR internalization and signalling. *Nature communications* **8**: 15054.
- Ben-Sahra I and Manning BD (2017) mTORC1 signaling and the metabolic control of cell growth. *Current opinion in cell biology* **45**: 72-82.
- Cahill TJ, Thomsen AR, Tarrasch JT, Plouffe B, Nguyen AH, Yang F, Huang L-Y, Kahsai AW, Bassoni DL and Gavino BJ (2017) Distinct conformations of GPCR- β -arrestin complexes mediate desensitization, signaling, and endocytosis. *Proceedings of the National Academy of Sciences*: 201701529.
- Cho C-H (2011) Frontier of epilepsy research-mTOR signaling pathway. *Experimental & molecular medicine* **43**(5): 231.
- Cvacek V, Goddard WA, 3rd and Abrol R (2016) Structure-Based Sequence Alignment of the Transmembrane Domains of All Human GPCRs: Phylogenetic, Structural and Functional Implications. *PLoS computational biology* **12**(3): e1004805.
- De Toni L, De Filippis V, Tesconi S, Ferigo M, Ferlin A, Scattolini V, Avogaro A, Vettor R and Foresta C (2014) Uncarboxylated osteocalcin stimulates 25-hydroxy vitamin D production in Leydig cell line through a GPRC6a-dependent pathway. *Endocrinology* **155**(11): 4266-4274.
- De Toni L, Di Nisio A, Speltra E, Rocca MS, Ghezzi M, Zuccarello D, Turiaco N, Ferlin A and Foresta C (2016) Polymorphism rs2274911 of GPRC6A as a novel risk factor for testis failure. *J Clin Endocrinol Metab* **101**(3): 953-961.
- Di Nisio A, Rocca MS, Fadini GP, De Toni L, Marcuzzo G, Marescotti MC, Sanna M, Plebani M, Vettor R and Avogaro A (2017) The rs2274911 polymorphism in GPRC6A gene is associated with insulin resistance in normal weight and obese subjects. *Clinical endocrinology* **86**(2): 185-191.
- Efeyan A, Zoncu R and Sabatini DM (2012) Amino acids and mTORC1: from lysosomes to disease. *Trends in molecular medicine* **18**(9): 524-533.
- Ferron M, Wei J, Yoshizawa T, Del Fattore A, DePinho RA, Teti A, Ducy P and Karsenty G (2010) Insulin signaling in osteoblasts integrates bone remodeling and energy metabolism. *Cell* **142**(2): 296-308.
- Foresta C, Strapazzon G, De Toni L, Giancesello L, Bruttocao A, Scarda A, Plebani M and Garolla A (2011) Androgens modulate osteocalcin release by human visceral adipose tissue. *Clin Endocrinol (Oxf)* **75**(1): 64-69.

- Gardner LA, Naren AP and Bahouth SW (2007) Assembly of an SAP97-AKAP79-cAMP-dependent protein kinase scaffold at the type 1 PSD-95/DLG/ZO1 motif of the human beta(1)-adrenergic receptor generates a receptosome involved in receptor recycling and networking. *J Biol Chem* **282**(7): 5085-5099.
- Iki M, Tamaki J, Fujita Y, Kouda K, Yura A, Kadowaki E, Sato Y, Moon JS, Tomioka K, Okamoto N and Kurumatani N (2012) Serum undercarboxylated osteocalcin levels are inversely associated with glycemic status and insulin resistance in an elderly Japanese male population: Fujiwara-kyo Osteoporosis Risk in Men (FORMEN) Study. *Osteoporosis international : a journal established as result of cooperation between the European Foundation for Osteoporosis and the National Osteoporosis Foundation of the USA* **23**(2): 761-770.
- Jacobsen SE, Ammendrup-Johnsen I, Jansen AM, Gether U, Madsen KL and Bräuner-Osborne H (2017) The GPRC6A receptor displays constitutive internalization and sorting to the slow recycling pathway. *J Biol Chem* **292**(17): 6910-6926.
- Jørgensen S, Have CT, Underwood CR, Johansen LD, Wellendorph P, Gjesing AP, Jørgensen CV, Quan S, Rui G and Inoue A (2017) Genetic variations in the human G protein-coupled receptor class C, group 6, member A (GPRC6A) control cell surface expression and function. *J Biol Chem* **292**(4): 1524-1534.
- Kapahi P, Chen D, Rogers AN, Katewa SD, Li PW-L, Thomas EL and Kockel L (2010) With TOR, less is more: a key role for the conserved nutrient-sensing TOR pathway in aging. *Cell metabolism* **11**(6): 453-465.
- Karsenty G and Olson EN (2016) Bone and Muscle Endocrine Functions: Unexpected Paradigms of Inter-organ Communication. *Cell* **164**(6): 1248-1256.
- Kinkade CW, Castillo-Martin M, Puzio-Kuter A, Yan J, Foster TH, Gao H, Sun Y, Ouyang X, Gerald WL, Cordon-Cardo C and Abate-Shen C (2008) Targeting AKT/mTOR and ERK MAPK signaling inhibits hormone-refractory prostate cancer in a preclinical mouse model. *The Journal of clinical investigation* **118**(9): 3051-3064.
- Ko E, Choi H, Kim B, Kim M, Park K-N, Bae I-H, Sung YK, Lee TR, Shin DW and Bae YS (2014) Testosterone stimulates Duox1 activity through GPRC6A in skin keratinocytes. *J Biol Chem* **289**(42): 28835-28845.
- Laplante M and Sabatini DM (2009) mTOR signaling at a glance. *Journal of cell science* **122**(20): 3589-3594.
- Laplante M and Sabatini DM (2012) mTOR signaling in growth control and disease. *Cell* **149**(2): 274-293.
- Lee NK, Sowa H, Hinoi E, Ferron M, Ahn JD, Confavreux C, Dacquin R, Mee PJ, McKee MD, Jung DY, Zhang Z, Kim JK, Mauvais-Jarvis F, Ducy P and Karsenty G (2007) Endocrine regulation of energy metabolism by the skeleton. *Cell* **130**(3): 456-469.
- Lefkowitz RJ and Shenoy SK (2005) Transduction of receptor signals by beta-arrestins. *Science* **308**(5721): 512-517.
- Li X, Nooh MM and Bahouth SW (2013) Role of AKAP79/150 protein in beta1-adrenergic receptor trafficking and signaling in mammalian cells. *JBiolChem* **288**(47): 33797-33812.

- Long Q-Z, Du Y-F, Ding X-Y, Li X, Song W-B, Yang Y, Zhang P, Zhou J-P and Liu X-G (2012) Replication and fine mapping for association of the C2orf43, FOXP4, GPRC6A and RFX6 genes with prostate cancer in the Chinese population. *PLoS one* **7**(5): e37866.
- Mendoza MC, Er EE and Blenis J (2011) The Ras-ERK and PI3K-mTOR pathways: cross-talk and compensation. *Trends in biochemical sciences* **36**(6): 320-328.
- Mera P, Laue K, Ferron M, Confavreux C, Wei J, Galan-Diez M, Lacampagne A, Mitchell SJ, Mattison JA, Chen Y, Bacchetta J, Szulc P, Kitsis RN, de Cabo R, Friedman RA, Torsitano C, McGraw TE, Puchowicz M, Kurland I and Karsenty G (2016) Osteocalcin Signaling in Myofibers Is Necessary and Sufficient for Optimum Adaptation to Exercise. *Cell Metab* **23**(6): 1078-1092.
- Norskov-Lauritsen L, Jorgensen S and Brauner-Osborne H (2015) N-glycosylation and disulfide bonding affects GPRC6A receptor expression, function, and dimerization. *FEBS letters* **589**(5): 588-597.
- Otani T, Mizokami A, Hayashi Y, Gao J, Mori Y, Nakamura S, Takeuchi H and Hirata M (2015) Signaling pathway for adiponectin expression in adipocytes by osteocalcin. *Cellular signalling* **27**(3): 532-544.
- Oury F, Ferron M, Huizhen W, Confavreux C, Xu L, Lacombe J, Srinivas P, Chamouni A, Lugani F and Lejeune H (2013) Osteocalcin regulates murine and human fertility through a pancreas-bone-testis axis. *The Journal of clinical investigation* **123**(6): 2421-2433.
- Pi M, Faber P, Ekema G, Jackson PD, Ting A, Wang N, Fontilla-Poole M, Mays RW, Brunden KR, Harrington JJ and Quarles LD (2005) Identification of a novel extracellular cation-sensing G-protein-coupled receptor. *J Biol Chem* **280**(48): 40201-40209.
- Pi M, Kapoor K, Wu Y, Ye R, Senogles SE, Nishimoto SK, Hwang DJ, Miller DD, Narayanan R, Smith JC, Baudry J and Quarles LD (2015) Structural and Functional Evidence for Testosterone Activation of GPRC6A in Peripheral Tissues. *Molecular endocrinology* **29**(12): 1759-1773.
- Pi M, Kapoor K, Ye R, Hwang DJ, Miller DD, Smith JC, Baudry J and Quarles LD (2018a) Computationally identified novel agonists for GPRC6A. *PLoS one* **13**(4): e0195980.
- Pi M, Kapoor K, Ye R, Nishimoto SK, Smith JC, Baudry J and Quarles LD (2016) Evidence for Osteocalcin Binding and Activation of GPRC6A in beta-Cells. *Endocrinology* **157**(5): 1866-1880.
- Pi M, Kapoor K, Ye R, Smith JC, Baudry J and Quarles LD (2018b) GPCR6A Is a Molecular Target for the Natural Products Gallate and EGCG in Green Tea. *Mol Nutr Food Res* **62**(8): e1700770.
- Pi M, Nishimoto SK and Quarles LD (2017) GPRC6A: Jack of all metabolism (or master of none). *Molecular metabolism* **6**(2): 185-193.
- Pi M, Parrill AL and Quarles LD (2010) GPRC6A mediates the non-genomic effects of steroids. *J Biol Chem* **285**(51): 39953-39964.
- Pi M and Quarles LD (2012) GPRC6A regulates prostate cancer progression. *The Prostate* **72**(4): 399-409.

- Pi M, Wu Y, Lenchik NI, Gerling I and Quarles LD (2012) GPRC6A mediates the effects of L-arginine on insulin secretion in mouse pancreatic islets. *Endocrinology* **153**(10): 4608-4615.
- Pi M, Wu Y and Quarles LD (2011) GPRC6A mediates responses to osteocalcin in β -cells in vitro and pancreas in vivo. *Journal of Bone and Mineral Research* **26**(7): 1680-1683.
- Pittas AG, Harris SS, Eliades M, Stark P and Dawson-Hughes B (2009) Association between serum osteocalcin and markers of metabolic phenotype. *J Clin Endocrinol Metab* **94**(3): 827-832.
- Robertson MJ, Deane FM, Robinson PJ and McCluskey A (2014) Synthesis of Dynole 34-2, Dynole 2-24 and Dyngo 4a for investigating dynamin GTPase. *Nature protocols* **9**(4): 851-870.
- Saxton RA and Sabatini DM (2017) mTOR signaling in growth, metabolism, and disease. *Cell* **168**(6): 960-976.
- Takata R, Akamatsu S, Kubo M, Takahashi A, Hosono N, Kawaguchi T, Tsunoda T, Inazawa J, Kamatani N and Ogawa O (2010) Genome-wide association study identifies five new susceptibility loci for prostate cancer in the Japanese population. *Nature genetics* **42**(9): 751.
- Thomsen AR, Plouffe B, Cahill III TJ, Shukla AK, Tarrasch JT, Dosey AM, Kahsai AW, Strachan RT, Pani B and Mahoney JP (2016) GPCR-G protein- β -arrestin super-complex mediates sustained G protein signaling. *Cell* **166**(4): 907-919.
- Tomaszewski M, Eales J, Denniff M, Myers S, Chew GS, Nelson CP, Christofidou P, Desai A, Busst C, Wojnar L, Musialik K, Jozwiak J, Debiec R, Dominiczak AF, Navis G, van Gilst WH, van der Harst P, Samani NJ, Harrap S, Bogdanski P, Zukowska-Szczechowska E and Charchar FJ (2015) Renal Mechanisms of Association between Fibroblast Growth Factor 1 and Blood Pressure. *Journal of the American Society of Nephrology : JASN* **26**(12): 3151-3160.
- Tsvetanova NG and von Zastrow M (2014) Spatial encoding of cyclic AMP signaling specificity by GPCR endocytosis. *Nature chemical biology* **10**(12): 1061-1065.
- Wei J, Hanna T, Suda N, Karsenty G and Ducy P (2014) Osteocalcin promotes β -cell proliferation during development and adulthood through Gprc6a. *Diabetes* **63**(3): 1021-1031.
- Wellendorph P and Bräuner-Osborne H (2009) Molecular basis for amino acid sensing by family CG-protein-coupled receptors. *British journal of pharmacology* **156**(6): 869-884.
- White JP, Gao S, Puppa MJ, Sato S, Welle SL and Carson JA (2013) Testosterone regulation of Akt/mTORC1/FoxO3a signaling in skeletal muscle. *Molecular and cellular endocrinology* **365**(2): 174-186.
- Ye R, Pi M, Cox JV, Nishimoto SK and Quarles LD (2017) CRISPR/Cas9 targeting of GPRC6A suppresses prostate cancer tumorigenesis in a human xenograft model. *Journal of experimental & clinical cancer research : CR* **36**(1): 90.
- Yoshii SR and Mizushima N (2017) Monitoring and measuring autophagy. *International journal of molecular sciences* **18**(9): 1865.

FOOTNOTES

Funding was provided by National Institutes of Health Grant R01-AR37308 and Americans
Diabetes Association Grant 1-13-BS-149-BR (to L. Darryl Quarles).

Figure legends

Figure 1. GPRC6A directly mediated in testosterone-induced mTORC1 activation. (A) RT-PCR analysis of AR and GPRC6A expression in PC-3 cells. 22Rv1 was employed as positive control for AR and GPRC6A expression human prostate cancer cell line. (B) Establishment of GPRC6A KO (B12) cell line by CRISPR/Cas9 system. Western blot analysis of GPRC6A protein level in WT PC-3 cells (WT, with Cas9 expression but no sgRNA insert) and GPRC6A KO (B12) cells. (C) Real-time PCR of GPRC6A expression in WT PC-3 or KO PC-3 cells. Data are presented as mean \pm SD of n=3, independent experiments each performed 6 replicates. Different letters in the superscripts above the data points indicate significant differences between groups. Values sharing the same superscript letters are not significantly different from each other, and values with different superscript letters indicate significant differences between groups ($p < 0.05$, Student's t test). (D) Knockout of GPRC6A abolished testosterone-induced mTORC1 activation. PC-3 WT cells and GPRC6A KO (B12) cells were treated with different concentration testosterone. Cells were incubated in HBSS buffer for 2 h before 20 min testosterone stimulation. Data are presented as mean \pm SD, N=3, independent experiments each performed in biological triplicates. Statistical differences between groups are indicated by superscript letters ($p < 0.05$, Two-way ANOVA with Tukey's multiple comparisons test), as described for Panel C. (E) PC-3 cells were incubated in HBSS buffer for 2 h before 20 min treatment with DHT at different concentration. No activation is seen by DHT treatment. Statistical differences between groups are indicated by superscript letters,

as described for Panel D. (F) Ca^{2+} is essential for the activation of mTORC1 and ERK and Akt phosphorylation. PC-3 cells were incubated in HBSS buffer with or without 0.5 mM Ca^{2+} for 2 h before 20 min testosterone stimulation. PC-3 cells were stimulated with HBSS buffer in the presence or absence of 0.5 mM Ca^{2+} . Statistical differences between groups are indicated by superscript letters, as described for Panel D.

Figure 2. Testosterone regulated mTORC1 signaling via ERK and Akt signaling. (A) Time dependence of testosterone activated mTORC1 signaling. PC-3 cells were assessed at different times after addition of testosterone at a concentration of 50 nM. Data are presented as mean \pm SD, n=3, independent experiments each performed in biological triplicates. Different letters in the superscripts above the data points indicate significant differences between groups. Values sharing the same superscript letters are not significantly different from each other, and values with different superscript letters indicate significant differences between groups ($p < 0.05$, Two-way ANOVA with Tukey's multiple comparisons test). (B) Time-dependent testosterone activation of ERK and AKT phosphorylation. PC-3 cells were incubated in HBSS buffer for 2 h before testosterone (50 nM) stimulation. ERK and AKT activation were analyzed by western blot. Statistical differences between groups are indicated by superscript letters, as described for Panel A. (C and D). Testosterone-induced mTORC1 signaling activation is inhibited by mTOR, AKT or ERK inhibitors. PC-3 cells in HBSS were treated with MK-2206 (MK, 1 mM) and/or ERK inhibitor PD98059 (PD, 10 μM), Rapamycin (RP, 100 nM) for 20 min, PC-3 cells

were incubated in HBSS buffer for 2 h before 20 min testosterone stimulation. Statistical differences between groups are indicated by superscript letters, as described for Panel A.

Figure 3. GPRC6A mediated in testosterone-induced cell proliferation and autophagy.

(A) Cell proliferation of PC-3 WT cells and KO (B12) cells using MTT method. 3×10^3 per well of cells were seed in 96-well plate at day 0. Cell viability was measured at day 2. Cells were cultured in complete RPMI 1640 media with or without 50 nM testosterone (T50). Data are the mean \pm SD, n=8. Different letters in the superscripts above the data points indicate significant differences between groups. Values sharing the same superscript letters are not significantly different from each other, and values with different superscript letters indicate significant differences between groups ($p < 0.05$, Two-way ANOVA with Tukey's multiple comparisons test). (B) Western analysis of cell proliferation marker Ki67 expression and mTORC1 activation. Cells were cultured in complete RPMI 1640 media with or without 50 nM testosterone (T50) for 48 h. (C) Time-course of testosterone on ULK1 activation. Phosphorylation of ULK1 at Ser757 were measured using western blot, PC-3 WT cells were incubated in HBSS buffer for 2 h before 20 min testosterone (50 nM, T50) stimulation. (D) Western blot analysis of LC3B level and ULK1 activation. Cell autophagy was induced by 5h starvation in HBSS with 50 μ M chloroquine (Lee et al., 2007). (E) Representative LC3 punctate images of PC-3 WT cells and PC-3 GPRC6A-KO (B12) cells stably expressing LC3-RFP. Autophagy is induced by 5h starvation in HBSS buffer with 50 μ M chloroquine (Lee et al., 2007) . The scale bar represents 20 μ m. LC3 punctate were quantitated by Image J

software. Data are mean \pm SD of LC3 punctate/cell. Statistical differences between groups are indicated by superscript letters, as described for Panel A.

Figure 4. Cellular compartmentalization of the various GPRC6A constructs in HEK-293

cells. (A) Distribution of the various GPRC6A constructs in HEK-293 cells. Fluorescence confocal microscopy of cells expressing the indicated GPR6A constructs that were either fixed (*images a, c, e*) or fixed and then permeabilized (*images b, d, f*). The distribution of pixels was obtained by confocal microscopy and the colors shown are *pseudo* colors, while the inset represents Nomarski images that were acquired at the same magnification. These images are representative of images derived from three separate experiments with 10 aggregate images per condition. The scale bar represents 5 μ m. (B) Digitized difference GPRC6A membrane location. Data are mean \pm SD of GPRC6A pixels outside a 300-nm partition derived from 30 images derived from n=3 experiments. Different letters in the superscripts above the data points indicate significant differences between groups. Values sharing the same superscript letters are not significantly different from each other, and values with different superscript letters indicate significant differences between groups ($p < 0.05$, Two-way ANOVA with Tukey's multiple comparisons test).

Figure 5. Comparison of intracellular function of mouse and human GPRC6A in HEK-

293 cells. (A) Dyngo-4a inhibited GPRC6A ligand, testosterone induced receptor internalization. The slides were pretreated with diluent or with 30 μ M Dyngo-4a for 30 min and

then exposed to 1 μ M testosterone for 30 min and fixed (*images c and d*, respectively). The scale bar represents 5 μ m. (B and C) Comparison of Dyngo-4a and Barbadin regulated GPRC6A-mediated ligand, testosterone induced ERK and S6K phosphorylation in HEK-293 cells stably transfected with WT mouse and human GPRC6A (mGPRC6A^{ICL3_KGRKLP} and hGPRC6A^{ICL3_KGKY}) cDNAs. Cells were preincubated with vehicle, Dyngo-4a (30 μ M (Abcam, Ab120689), or Barbadin (10 μ M) (Axon Medchem, Axon2774) for 20 min after testosterone (T) treatment. (D) Comparison of dimerization of the various GPRC6As in HEK-293 cells, WT mouse GPRC6A (mGPRC6A^{ICL3_KGRKLP}) versus the “humanized” mouse GPRC6A (mGPRC6A^{ICL3_KGRKLP}) or human GPRC6A (hGPRC6A^{ICL3_KGKY}) analyzed by Western blots. 16 μ g each plasmid cDNAs were transfected into HEK-293 cells (1.5×10^6 cells/100mm dish), and 100 μ g each total protein samples were loaded on 3-8% SDS page gels, anti-Myc antibody were used for Western blot analysis. These images are representative of images derived from three separate experiments.

Figures

Figure 1

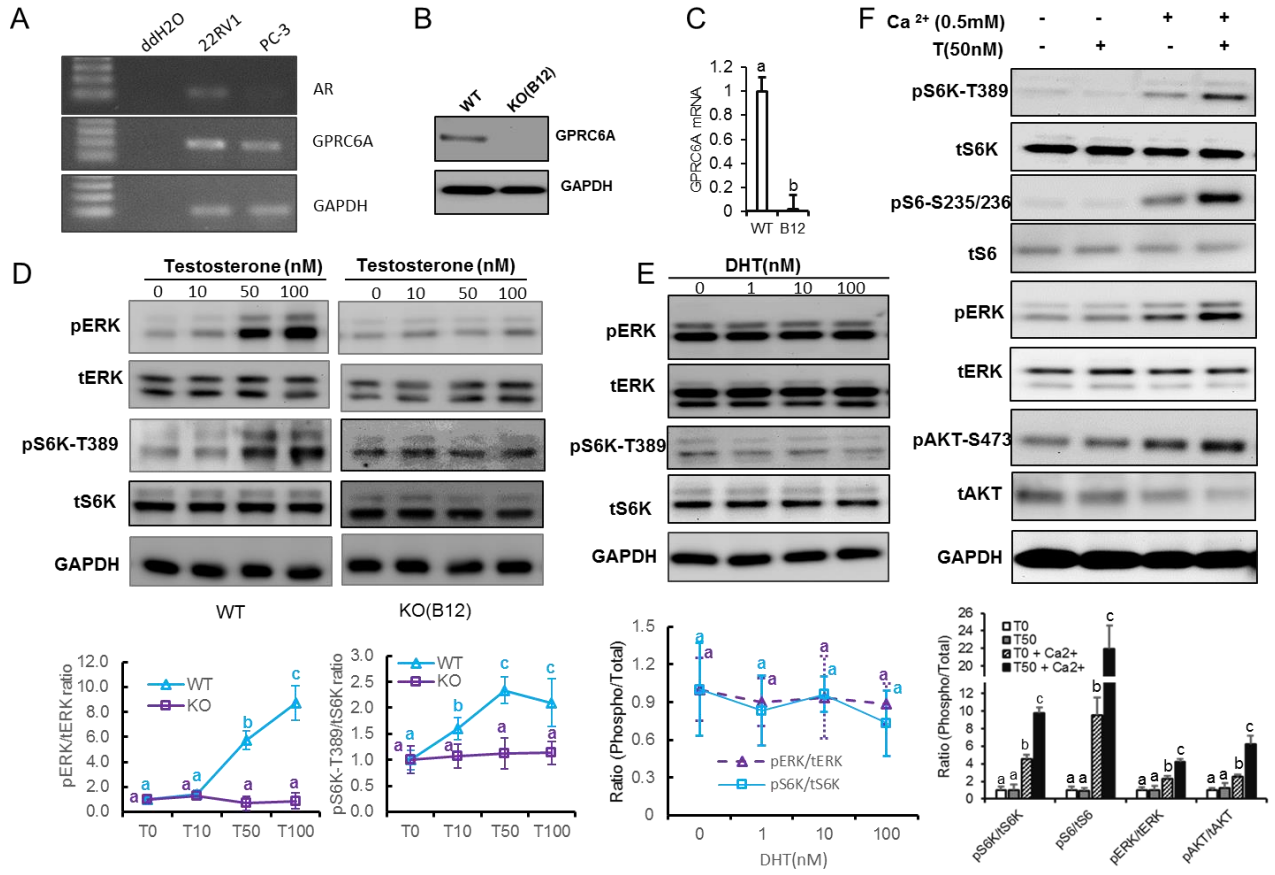


Figure 2

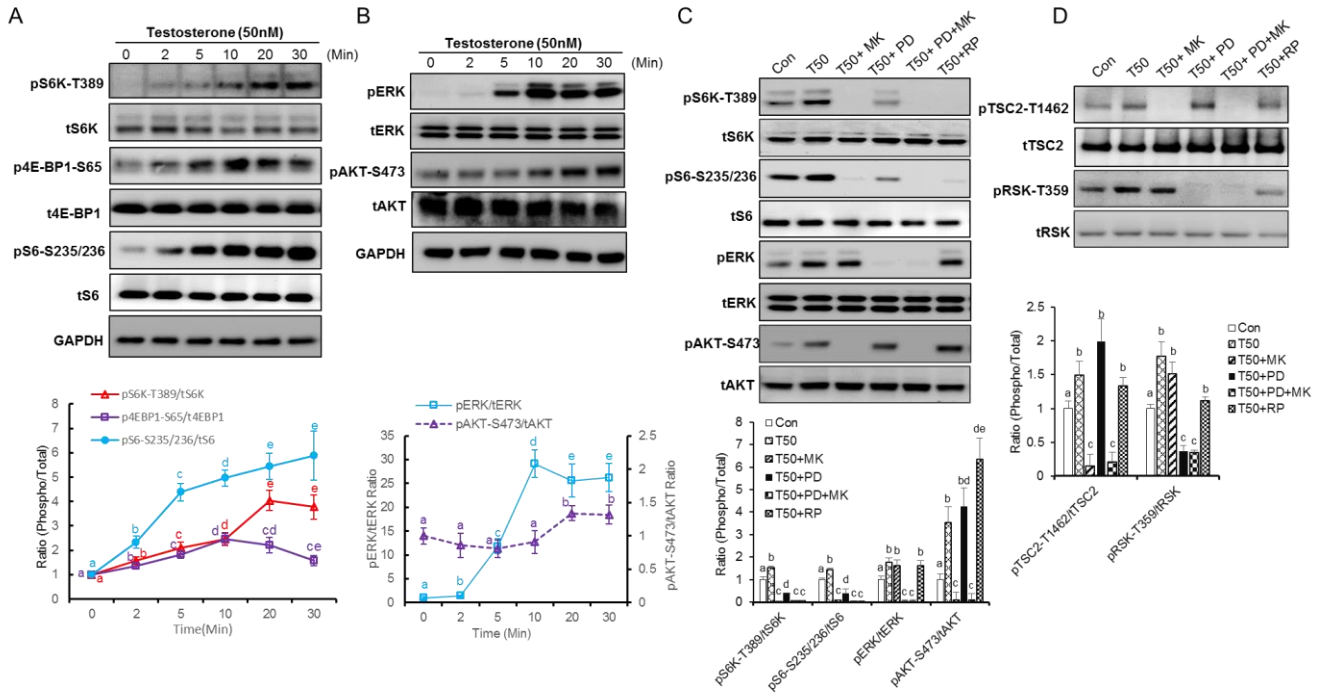


Figure 3

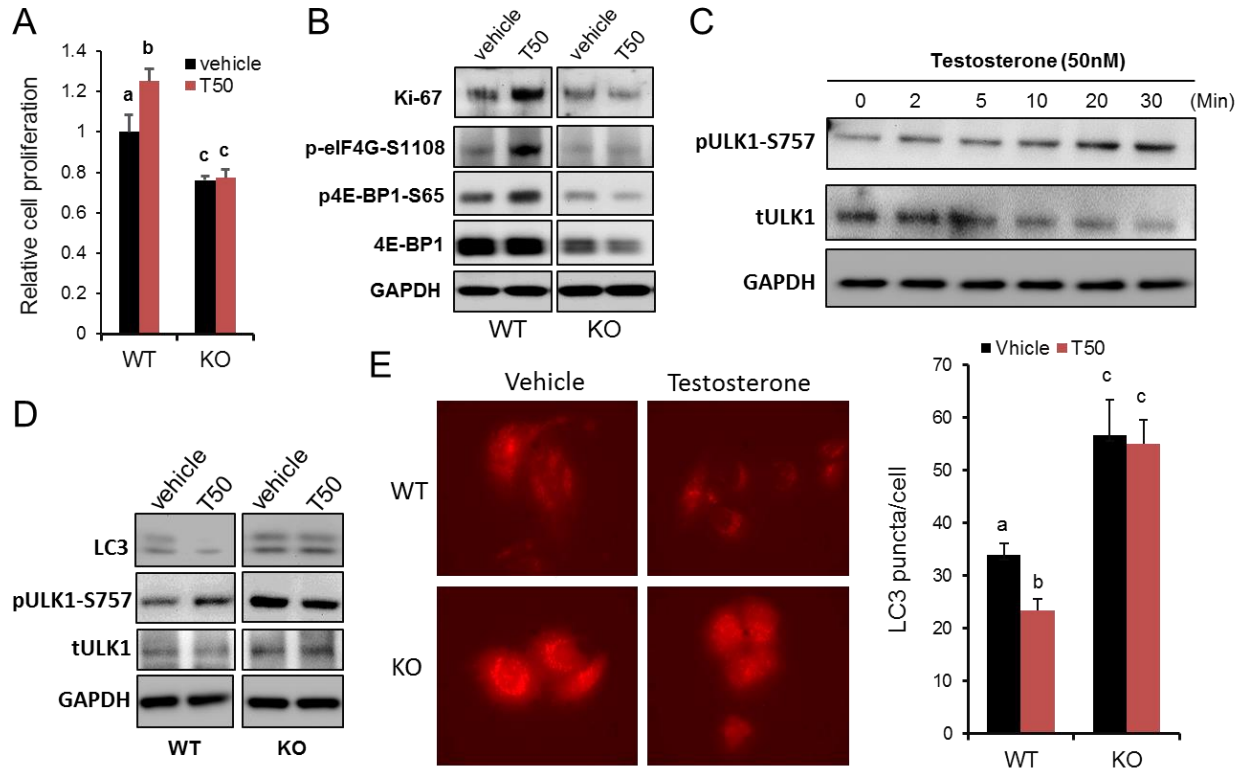


Figure 4

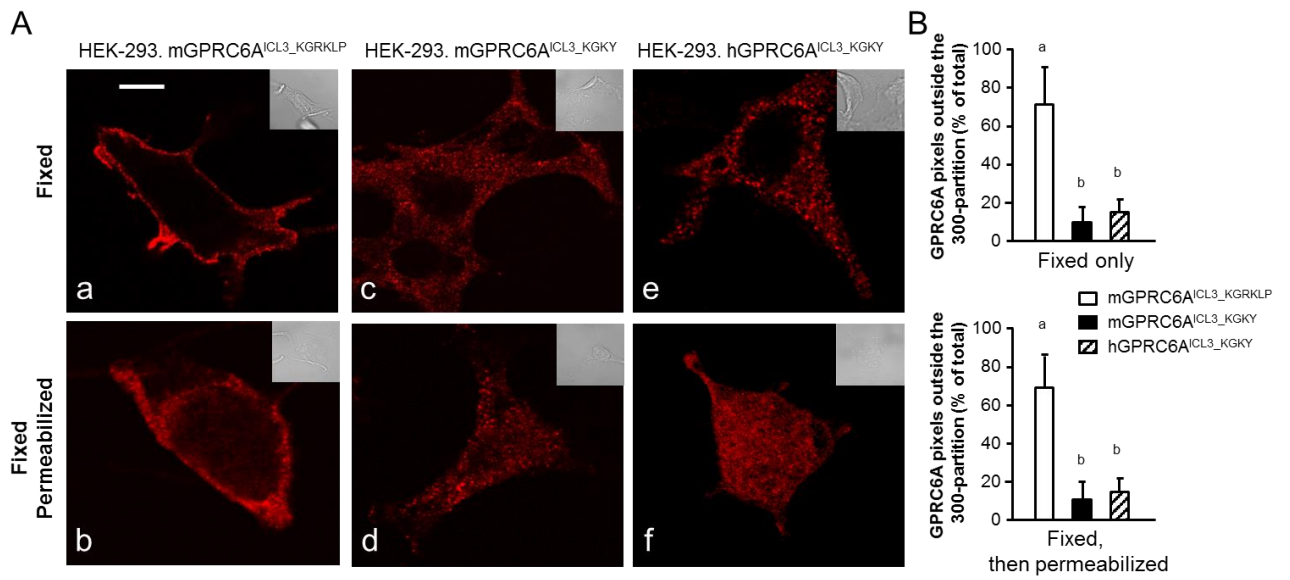


Figure 5

